JHEP

Published for SISSA by Springer

Received: *February 21, 2018*
Revised: *April 18, 2018*
Accepted: *May 4, 2018*
Published: *May 9, 2018*

Probing neutrino coupling to a light scalar with coherent neutrino scattering

Yasaman Farzan,[a] **Manfred Lindner,**[b] **Werner Rodejohann**[b] **and Xun-Jie Xu**[b]

[a] *Institute for Research in Fundamental Sciences (IPM), P.O. Box 19395-5531, Tehran, Iran*
[b] *Max-Planck-Institut für Kernphysik, Postfach 103980, D-69029 Heidelberg, Germany*

E-mail: yasaman@theory.ipm.ac.ir, lindner@mpi-hd.mpg.de, werner.rodejohann@mpi-hd.mpg.de, xunjie@mpi-hd.mpg.de

Abstract: Large neutrino event numbers in future experiments measuring coherent elastic neutrino nucleus scattering allow precision measurements of standard and new physics. We analyze the current and prospective limits of a light scalar particle coupling to neutrinos and quarks, using COHERENT and CONUS as examples. Both lepton number conserving and violating interactions are considered. It is shown that current (future) experiments can probe for scalar masses of a few MeV couplings down to the level of 10^{-4} (10^{-6}). Scalars with masses around the neutrino energy allow to determine their mass via a characteristic spectrum shape distortion. Our present and future limits are compared with constraints from supernova evolution, Big Bang nucleosynthesis and neutrinoless double beta decay. We also outline UV-complete underlying models that include a light scalar with coupling to quarks for both lepton number violating and conserving coupling to neutrinos.

Keywords: Beyond Standard Model, Neutrino Physics

ArXiv ePrint: 1802.05171

Open Access, © The Authors.
Article funded by SCOAP[3].

https://doi.org/10.1007/JHEP05(2018)066

JHEP05(2018)066

Contents

JHEP05(2018)066

1 Introduction

The observation of Coherent Elastic neutrino-Nucleus Scattering (CEνNS) by the COHERENT experiment [1] has opened a new window to probe Standard Model and beyond the Standard Model physics. Those include the determination of the Weinberg angle at low energies [2], nuclear physics parameters [3], searches for a magnetic moment of the neutrino [4, 5], for light sterile neutrinos [6–9], or for neutrino exotic interactions, be it the vector type [2, 10–17] or of other Lorentz-invariant types [13, 18]. In the near future, more experiments will be able to observe CEνNS, including CONUS [19], TEXONO [20], CONNIE [21], MINER [22], νGEN [23], Ricochet [24], and ν-cleus [25].

In the present paper we focus on new neutrino physics caused by a new light scalar. Such a particle can participate in coherent neutrino-nucleus scattering, and interestingly modify the nuclear recoil spectrum in a characteristic manner, both for a light scalar as well as heavy one. Most of our study will focus on the light scalar case. Light new physics is of course motivated by the lack of signals in collider experiments, and its consequences in coherent neutrino-nucleus scattering have been mentioned before [14–16, 26–29]. Mostly it was used that light physics does not suffer from limits on neutrino non-standard interactions

from high energy scattering experiments such as CHARM-II, as stressed in [30, 31]. Discovery limits on light particles in CEνNS have been discussed in refs. [14, 26, 29], indicating already before the observation by COHERENT that CEνNS could provide strong constraints on light mediators. In our work, as mentioned before, we focus on a new scalar particle and obtain the current limits from COHERENT on its mass and coupling with SM particles. We also consider explicit future realizations of this experiment and also of CONUS, which will use reactor antineutrinos to probe coherent scattering. The characteristic distortion of the spectrum shape for light scalars with masses around the neutrino energy allows to reconstruct the scalar mass, which we explicitly demonstrate. We also compare our limits with existing ones from a variety of sources in particle and astroparticle physics. UV-complete models that may be behind the existence of such light scalar particles are also outlined.

This paper is organized as follows: in section 2, we present the framework of a light scalar with couplings to neutrinos and quarks, discuss the coherent scattering cross section and include a discussion of form factors when the coupling to nucleons is considered. In section 3, we discuss the constraints on such scalar particles from various particle and astroparticle physics observables. In sections 4 and 5 we discuss and interpret the implications of various possible observations. In section 6, we summarize our findings. The calculational details and outlines for UV-complete gauge invariant models are presented in appendices.

2 Light scalar interactions in coherent neutrino-nucleus scattering

In this section, we first introduce the possible interactions of neutrinos with quarks (or nuclei) mediated by a light scalar boson and then discuss the corresponding cross section of coherent neutrino-nucleus scattering.

2.1 New scalar interactions

We consider a scalar field denoted by ϕ which couples to neutrinos. There are two possibilities for such coupling, namely lepton number violating (LNV) and conserving (LNC) couplings. The latter possibility requires the presence of right-handed neutrinos:

$$\mathcal{L}_{\rm LNC} \equiv \bar{\nu}\left(C_\nu + iD_\nu\gamma_5\right)\nu\phi = y_\nu\phi\bar{\nu}_R\nu_L + \text{H.c.}, \tag{2.1}$$

where $y_\nu = C_\nu - iD_\nu$. For simplicity, throughout this paper we implicitly assume that ϕ is a real field but most discussion and overall behavior of the bounds and limits remains valid for a complex ϕ as well. For real ϕ, the hermicity of the Lagrangian implies that C_ν and D_ν are real. Note that the couplings have flavor indices, suppressed here for clarity. The lepton number violating form of the interaction can be written in analogy as

$$\mathcal{L}_{\rm LNV} \equiv \frac{y_\nu}{2}\phi\bar{\nu}_L^c\nu_L + \text{H.c} = \frac{y_\nu}{2}\phi\nu_L^T C\nu_L + \text{H.c.} \tag{2.2}$$

In both Lagrangians y_ν can in general be a complex number.

The same scalar field can couple to quarks. Since in coherent neutrino scattering we are concerned with the effective coupling of ϕ with the whole nucleus N we write the Lagrangian as:

$$\mathcal{L}_{N\phi} \equiv \overline{\psi_N}\Gamma_{N\phi}\psi_N\phi, \tag{2.3}$$

JHEP05(2018)066

where ψ_N is the Dirac spinor of the nucleus, assuming it is a spin-1/2 particle.[1] We can write

$$\Gamma_{N\phi} \equiv C_N + D_N i\gamma^5. \tag{2.4}$$

Again, for real ϕ hermicity of the Lagrangian demands C_N and D_N to be real numbers. The conversion from fundamental quark couplings (C_q, D_q) to the effective coupling (C_N, D_N) will be discussed later. Note that we here consider both scalar and pseudo-scalar interactions. In what follows, the latter contribution is usually very much suppressed, and essentially only the scalar contribution is what matters.

In summary, the Lagrangian (in addition to the SM) responsible for coherent neutrino scattering is

$$\mathcal{L} \supset \mathcal{L}_{\nu\phi} + \mathcal{L}_{N\phi} - \frac{1}{2}m_\phi^2\phi^2 - M\overline{\psi_N}\psi_N, \tag{2.5}$$

where $\mathcal{L}_{\nu\phi}$ can be either eq. (2.1) or eq. (2.2). The masses of the scalar and nucleus are respectively denoted by m_ϕ and M. In appendix A, we present examples in which couplings to neutrinos and quarks can be embedded in electroweak symmetric models.

2.2 Cross section

The first thing to notice is that the Yukawa interaction of both LNC and LNV forms (either eq. (2.1) or eq. (2.2)) leads to chirality-flipping scattering which will not interfere with chirality-conserving SM weak interactions.[2] Thus, one can separate the cross section into two parts containing the pure SM and the new physics contributions:

$$\frac{d\sigma}{dT} = \frac{d\sigma_{\rm SM}}{dT} + \frac{d\sigma_\phi}{dT}, \tag{2.6}$$

where T denotes the recoil energy. The SM cross section, assuming full coherence is given by [33]

$$\frac{d\sigma_{\rm SM}}{dT} = \frac{G_F^2 M\left[N-(1-4s_W^2)Z\right]^2}{4\pi}\left(1-\frac{T}{T_{\rm max}}\right), \text{ where } T_{\rm max}(E_\nu) = \frac{2E_\nu^2}{M+2E_\nu}. \tag{2.7}$$

The coherent scattering mediated by the light scalar, independent of whether the new scalar interaction is of the LNC or LNV form, is (the derivation is given in appendix B):

$$\frac{d\sigma_\phi}{dT} = \frac{MY^4A^2}{4\pi(2MT+m_\phi^2)^2}\left[\frac{MT}{E_\nu^2} + \mathcal{O}\left(\frac{T^2}{E_\nu^2}\right)\right], \tag{2.8}$$

where we have defined

$$Y^4 \equiv \frac{C_N^2}{A^2}|y_\nu|^2. \tag{2.9}$$

Here C_N is the coupling of the scalar with the nucleus, whose connection to the fundamental quark couplings is discussed in the next subsection. The division by the atomic number

[1] The actual spin of the nucleus can take other values but the difference of the cross section is suppressed by E_ν^2/M^2 — see the appendix in [13].

[2] More generally, as it has been studied in [32], there is no interference in neutrino scattering between vector (or axial-vector) form interactions and other forms of interactions, including (pseudo-)scalar and tensor.

JHEP05(2018)066

in the definition of Y makes it almost independent of the type of nucleus — cf. eq. (2.19) and eq. (2.20). The cross section has little dependence[3] on D_N because the pseudo-scalar contribution is suppressed by the $\mathcal{O}\left(T^2/E_\nu^2\right)$ term. This is in analogy to dark matter direct detection where dark matter nucleon interactions mediated by a pseudo-scalar is well known to be suppressed.

Obviously scalar interactions lead to a spectral shape different from that in the SM case, see e.g. [13], where an effective scalar interaction, corresponding to $m_\phi^2 \gg MT$, is considered. For a light scalar under discussion here we see that additional modifications of the spectrum are possible, in particular if the scalar mass is of the same order or smaller than the typical momentum transfer $MT \sim E_\nu^2$.

2.3 From the fundamental couplings to the effective couplings

The effective couplings C_N and D_N originate from fundamental couplings of ϕ with the quarks. The connection between the effective couplings and the fundamental couplings has been well studied in spin-independent dark matter direct detection. Essentially, one needs to know the scalar form factors of quarks in the nuclei. We refer to [34] for the details and summarize the relevant results below.

Since the pseudo-scalar coupling D_N has no effect on CEνNS [cf. eq. (2.9)], we focus on the scalar coupling, C_N. Taking the fundamental scalar interaction of quarks with ϕ to be of the form

$$\mathcal{L} \supset \sum_q C_q \bar{q} q \phi, \tag{2.10}$$

the effective coupling C_N is related to C_q by

$$C_N = Z C_p + (A - Z) C_n, \tag{2.11}$$

where the couplings to protons and neutrons are

$$C_p = m_p \left[\sum_q C_q \frac{f_q^p}{m_q}\right], \; C_n = m_n \left[\sum_q C_q \frac{f_q^n}{m_q}\right]. \tag{2.12}$$

Here $m_p = 938.3\,\text{MeV}$ and $m_n = 939.6\,\text{MeV}$ are masses of proton and neutron; Z and $A-Z$ are proton and neutron numbers in the nucleus; m_q are quark masses; f_q^p and f_q^n are the scalar form factors in protons and neutrons. According to the updated data for the u and d quarks from [35, 36] and the data for the s quark from [37], the form factors are:

$$\begin{aligned} &f_d^p = 0.0411 \pm 0.0028, \qquad f_u^p = 0.0208 \pm 0.0015, \qquad f_s^p = 0.043 \pm 0.011, \\ &f_c^p \approx f_b^p \approx f_t^p \approx \frac{2}{27}(1 - f_d^p - f_u^p - f_s^p) \approx 0.066, \end{aligned} \tag{2.13}$$

$$\begin{aligned} &f_d^n = 0.0451 \pm 0.0027, \qquad f_u^n = 0.0189 \pm 0.0014, \qquad f_s^n = 0.043 \pm 0.011, \\ &f_c^n \approx f_b^n \approx f_t^n \approx \frac{2}{27}(1 - f_d^n - f_u^n - f_s^n) \approx 0.066, \end{aligned} \tag{2.14}$$

[3]The explicit form of the negligible term $\mathcal{O}\left(T^2/E_\nu^2\right)$ is actually $\left(1 + D_N^2/C_N^2\right)\frac{T^2}{2E_\nu^2}$ — see eq. (B.6) in the appendix.

JHEP05(2018)066

where $f_{c,b,t}$ are approximately the same for the heavy quarks because their contributions come from heavy quark loops that couple ϕ to the gluons [38]. The form factors computed by the effective field theory in refs. [39, 40] agree well with the above results. Notice that despite the different quark content, the couplings of proton and neutron to the scalar turn out to be almost equal: $|(C_n - C_p)/C_n| = \mathcal{O}(10\%)$. If C_q for the heavy quarks are of the same order of magnitude as for the light quarks, then the contributions of heavy quarks are negligible due to suppression by their masses. However, if $C_q \propto m_q$ (as in the case that the ϕ coupling to the quarks comes from the mixing of a scalar singlet with the SM Higgs), the contribution from all flavors will be comparable. Taking the following quark masses [41]:

$$\begin{aligned} &m_d = 4.7\,\text{MeV}, && m_u = 2.2\,\text{MeV}, && m_s = 96\,\text{MeV}, \\ &m_c = 1.27\,\text{GeV}, && m_b = 4.18\,\text{GeV}, && m_t = 173.2\,\text{GeV}, \end{aligned}$$

we obtain

$$\begin{aligned} m_p &\left(\frac{f_d^p}{m_d}, \frac{f_u^p}{m_u}, \frac{f_s^p}{m_s}, \frac{f_c^p}{m_c}, \frac{f_b^p}{m_b}, \frac{f_t^p}{m_t}\right) \\ &\approx (8.2,\, 8.9,\, 0.42,\, 4.9\times10^{-2},\, 1.5\times10^{-2},\, 3.6\times10^{-4})\,, \end{aligned} \tag{2.15}$$

$$\begin{aligned} m_n &\left(\frac{f_d^n}{m_d}, \frac{f_u^n}{m_u}, \frac{f_s^n}{m_s}, \frac{f_c^n}{m_c}, \frac{f_b^n}{m_b}, \frac{f_t^n}{m_t}\right) \\ &\approx (9.0,\, 8.1,\, 0.42,\, 4.9\times10^{-2},\, 1.5\times10^{-2}, 3.6\times10^{-4})\,. \end{aligned} \tag{2.16}$$

For Ge and CsI targets, taking the average values of $(Z,\, A)$ as (32, 72.6) and (54, 130), we can evaluate the explicit dependence of C_N on the C_q:

$$C_N = \begin{cases} 10^2 \times (6.3\,C_d + 6.1\,C_u) + (30.5\,C_s + 3.5\,C_c + 1.1\,C_b + 2.5\times10^{-2}\,C_t) & \text{(Ge)} \\ 10^3 \times (1.1\,C_d + 1.1\,C_u) + (54.7\,C_s + 6.3\,C_c + 1.9\,C_b + 4.7\times10^{-2}\,C_t) & \text{(CsI)} \end{cases}. \tag{2.17}$$

This means that from the fundamental coupling to the effective coupling an amplification by a factor of $\mathcal{O}(10^2)$ or $\mathcal{O}(10^3)$ can be present. The definition of Y in eq. (2.9), in terms of the fundamental couplings, can be rewritten as

$$Y \equiv \sqrt{\frac{|C_N y_\nu|}{A}} = \sqrt{\left|\left(\frac{A-Z}{A}\,C_n + \frac{Z}{A}\,C_p\right) y_\nu\right|}. \tag{2.18}$$

The dependence of Y on the types of targets is weak because for heavy nuclei, $\frac{A-Z}{A}$ and $\frac{Z}{A}$ are typically close to 1/2. For example, taking the average values of $(Z,\, A)$ for Ge and CsI targets, we get

$$Y_{\text{Ge}} \approx \sqrt{|(0.56\,C_n + 0.44\,C_p) y_\nu|}\,, \tag{2.19}$$

$$Y_{\text{CsI}} \approx \sqrt{|(0.58\,C_n + 0.42\,C_p) y_\nu|}\,. \tag{2.20}$$

When comparing the sensitivities of CEνNS experiments using different targets, we will ignore the small difference and assume $Y_{\text{Ge}} \approx Y_{\text{CsI}}$.

JHEP05(2018)066

3 Existing bounds from particle and astroparticle physics

In this section we review the relevant bounds on C_n, y_ν or on their product $(C_n y_\nu)$ from various observations and experiments other than coherent scattering. As we shall see, the bounds on the hadronic couplings are on $C_n = \mathcal{R}[\Gamma_{n\phi}]$ (not on D_n) but the bounds on neutrino couplings are on $|y_\nu|^2 = C_\nu^2 + D_\nu^2$. The difference originates from the fact that while nuclei in the considered setups are non-relativistic, neutrinos are ultra-relativistic.

- **Bounds on C_n from neutron nucleus scattering:** in the mass range of our interest, the strongest bounds on C_n come from low energy neutron scattering off nuclei [42–44], in particular using Pb as target. The effect of a new scalar would be to provide a Yukawa-type scattering potential whose effect can be constrained. Notice that like the case of CEνNS, since in these setups the nuclei are non-relativistic, their dominant sensitivity is only to C_n (not to D_n).

- **Bounds on y_ν from meson decay:** if the new light boson couples to neutrinos, it can open new decay modes for mesons such as $K^+ \to l^+\nu\phi$ or $\pi^+ \to l^+\nu\phi$. The scalar will eventually decay into a neutrino pair appearing as missing energy. From the absence of a signal for such decay modes, bounds of order 10^{-3} on $(\sum_\alpha |y_\nu|^2_{e\alpha})^{1/2}$ and $(\sum_\alpha |y_\nu|^2_{\mu\alpha})^{1/2}$ have been found from different modes [45]. Notice that as long as the mass of ϕ is much smaller than the meson mass the bound is independent of m_ϕ. Moreover, the bound similarly applies for the LNV and LNC cases. In the LNC case, sensitivity is to the combination $|y_\nu|^2 = C_\nu^2 + D_\nu^2$.

- **Bounds from double beta decay:** a LNV coupling of form $\phi\nu_e^T C\nu_e$ can cause neutrinoless double beta decay [46] in the form of $n+n \to p+p+e^-+e^-+\phi$, of course provided that ϕ is lighter than the Q value of the decaying nucleus. From double beta decay of ^{136}Xe with a Q value of 2.4 MeV the following bound is found [47]:

$$(y_\nu)_{ee} < 10^{-5}. \tag{3.1}$$

  A more recent and a bit weaker bound for $m_\phi < 2.03\,\text{MeV}$ comes from ^{76}Ge double beta decay [48].

- **Supernova bounds and limits:** light particles coupled to neutrinos and neutrons can affect the dynamics of a proto-neutron star in several ways. Before discussing the impact of our particular scenario on supernovae, let us very briefly review the overall structure of the core of a proto-neutron star in the first few 10 seconds after explosion when neutrinos are trapped inside the core (i.e., the mean free path of neutrinos is much smaller than the supernova core radius). For more details, the reader can consult the textbook [49]. In the first ~ 10 sec after collapse, the core has a radius of $\sim$ few 10 km and a matter density of $\rho \sim 10^{14}\,\text{g cm}^{-3}$ (comparable to nuclear density). However, because of the high pressure, most of the nucleons are free. As mentioned before, neutrinos are trapped inside the core and are thermalized with a temperature of $\sim 10\,\text{MeV}$. The core can be hypothetically divided into the inner core with a radius

JHEP05(2018)066

of 10-15 km and the outer core. Within the inner core, the chemical potential of the ν_e is about 200 MeV which is much larger than their temperature, implying that ν_e are degenerate. The chemical potentials of ν_μ and ν_τ are zero and their temperatures are equal. Thus, inside the inner core $n_{\bar{\nu}_e} \ll n_{\nu_\mu} = n_{\bar{\nu}_\mu} = n_{\nu_\tau} = n_{\bar{\nu}_\tau} \ll n_{\nu_e}$, where n_{ν_α} is the number density of ν_α. In the outer core, the chemical potential of ν_e decreases and the number densities of ν_e and $\bar{\nu}_e$ are almost equal. Notice that the average energies of ν_μ, ν_τ and their antiparticles throughout the core are given by their temperature which is of order of few 10 MeV. The energies of ν_e and $\bar{\nu}_e$ in the outer core, where the chemical potential vanishes, are also of the same order but the energy of ν_e in the inner core is of order of the chemical potential, 200 MeV. The neutrinos scatter off nucleons with a cross section of $\sigma \sim G_F^2 E_\nu^2/(4\pi)$. Considering the high density of nucleons, the mean free path for neutrinos will be of order of $\lambda \simeq 300$ cm, which is much smaller than the core radius $R \sim$ few 10 km. The diffusion time, given by $R(R/\lambda)$, is therefore of order of $\mathcal{O}(1$ sec) to $\mathcal{O}(10$ sec). Neutrinos diffusing out of the core carry out the binding energy of the star which is of order of 10^{53} erg.

Let us now see how new light particles coupled to neutrinos and matter fields can affect this picture. First, let us discuss the impact on supernova cooling. If the interaction of the new particle is very feeble, it cannot be trapped. Thus, if it is produced inside the core it can exit without hinderance and take energy out of the core leaving no energy for neutrinos to show up as the observed events of SN1987a. This sets an upper bound on the coupling of the new particles. On the other hand, if the coupling is large enough to trap the new particles, the impact on cooling will not be dramatic. Still, if the new particles are stable, they can diffuse out and, along with neutrinos, can contribute to supernova cooling. Considering however the theoretical uncertainty in the evaluation of total binding energy and the observational uncertainty on the energy carried away, such contributions can be tolerated. Thus, supernova cooling consideration, within present uncertainties, can only rule out a range of coupling between an upper bound and a lower bound. New interactions can also affect the mean free path of neutrinos λ and therefore the diffusion time R^2/λ, which roughly speaking coincides with the observable duration of neutrino emission from a supernova. This sets another limit. Finally, if there is a new process that can remove ν_e and/or convert it to any of $\bar{\nu}_e$, $\nu_{\mu(\tau)}$ or $\bar{\nu}_{\mu(\tau)}$, it can have profound effect on the Equation of State (EoS) in the inner core. For example, if ν_e (with energy of 200 MeV) are converted to ν_μ, the temperature of ν_μ will increase dramatically. Conversion of ν_e to $\bar{\nu}_e$ will lead to the production of e^+ which annihilates with electrons inside the core.

In our case the ϕ particles can decay into a neutrino pair. The decay length is evaluated to be approximately $(10^{-5}/|y_\nu|)^2(E_\phi/10\text{ MeV})(5\text{ MeV}/m_\phi)^2$ cm, which is much smaller than the radius of the proto-neutron star ($\sim$ few 10 km). The consequences of new interactions on supernova explosions can be categorized into three effects: (1) change of equation of state in case of LNV interaction; (2) new cooling modes because of right-handed (anti)neutrino emission in case of LNC interaction; (3) prolonging the duration of neutrino emission (R^2/λ) because of a shorter mean free path λ. In

JHEP05(2018)066

all these three effects, the neutrino scattering plays a key role. Neglecting flavor indices, we find that the neutrino-neutrino scattering cross section is comparable to the ν-nucleon scattering cross section if $y_\nu \sim C_n$. The number density of nucleons is larger than that of neutrinos, thus the ν-nucleon scattering should be more important. The cross section of the scattering due to ϕ both for LNV and LNC cases can be estimated as

$$\sigma(\overset{(-)}{\nu} + n \to \overset{(-)}{\nu} + n) = \frac{|y_\nu|^2 C_n^2}{16\pi E_\nu^2}\left[\log\frac{4E_\nu^2 + m_\phi^2}{m_\phi^2} - \frac{4E_\nu^2}{4E_\nu^2 + m_\phi^2}\right]. \tag{3.2}$$

The scattering cross section for sterile (anti)neutrinos is given by the same formula.

Let us discuss the three effects mentioned above one by one. If ν_e has a LNV coupling to ϕ of the form $(y_\nu)_{e\alpha}\phi\nu_e^T C\nu_\alpha$, where $\alpha \in \{e, \mu, \tau\}$, ν_e can be converted into $\bar{\nu}_\alpha$. The produced antineutrino will be trapped. However, if

$$\sigma(\nu_e + n \to \bar{\nu}_\alpha + n) \times \frac{\rho}{m_n} \times (10\text{ sec}) \gtrsim 1, \tag{3.3}$$

a significant fraction of degenerate ν_e in the inner core will convert into antineutrinos, drastically changing the equation of state. That is, for

$$\sqrt{(y_\nu)_{e\alpha} C_n} > 2 \times 10^{-7} \sqrt[4]{\frac{E_\nu^2}{\log\frac{4E_\nu^2+m_\phi^2}{m_\phi^2} - \frac{4E_\nu^2}{4E_\nu^2+m_\phi^2}}}, \tag{3.4}$$

in which $E_{\nu_e} \sim 200\,\text{MeV}$, the equation of state of the supernova core has to be reconsidered. In subsequent plots that summarize the limits on our scenario, we call the associated limit to avoid this feature as "SN core EoS". Since the temperatures of ν_μ and ν_τ are expected to be the same and their chemical potentials to be zero, conversion of ν_μ and ν_τ to $\bar{\nu}_\mu$ and $\bar{\nu}_\tau$ due to non-zero $(y_\nu)_{\mu\mu}$, $(y_\nu)_{\mu\tau}$ and $(y_\nu)_{\tau\tau}$ will not change the equation of state.

When the interaction is LNC, scattering will convert left-handed neutrinos (right-handed antineutrinos) into sterile right-handed neutrinos (left-handed antineutrinos), which do not participate in weak interactions. If $\sigma(\rho/m_n)(10\,\text{sec}) \gtrsim 1$, a significant fraction of the active (anti)neutrinos will convert into sterile ones. Avoiding this generates an upper limit on the coupling. If $\sigma(\rho/m_n)R \gtrsim 100$, the produced sterile neutrinos will be trapped. The values of $\sqrt{y_\nu C_n}$ between these two limits are therefore excluded by supernova cooling considerations. The limits are denoted in figure 4 as "SN energy loss" and "SN ν_R trapping", respectively.

Drawing these figures we have assumed a nominal temperature of 30 MeV for neutrinos which is the typical energy for all neutrinos in the outer core. In case that the neutrino-nucleon scattering cross section due to ϕ exchange becomes comparable to the standard weak cross section $G_F^2 E_\nu^2/(4\pi)$, the diffusion time R^2/λ will be significantly affected. This limit is shown in figures 4 and 5 as "SN ν diffusion", and holds for both the LNC and LNV cases.

JHEP05(2018)066

- **BBN and CMB bounds:** the contribution from the LNC and LNV cases to the additional number of relativistic degrees of freedom ($\delta N_{\rm eff}$) will be quite different so in the following, we address them separately.

  i) LNV case: in this case, no ν_R exist so we should only check for the ϕ production. For $m_\phi \gtrsim 1\,\text{MeV}$, ϕ will be produced at high temperatures but it will decay before neutrino decoupling without affecting $N_{\rm eff}$ at the BBN or the CMB era. Thus, within the present uncertainties, there is no bound from BBN for $m_\phi \gtrsim 1\,\text{MeV}$. Lighter ϕ, in turn, can contribute to $N_{\rm eff}$ as one scalar degree of freedom if they enter thermal equilibrium. Taking $n_\nu \sigma(\nu\nu \to \phi) H^{-1}|_{T=1\,\text{MeV}} < 1$, we find

$$|y_\nu| < 5 \times 10^{-9} \frac{m_\phi}{\text{MeV}}. \tag{3.5}$$

  Notice that for $0.1\ \text{MeV} < m_\phi < 1\ \text{MeV}$, although ϕ decays away before the onset of BBN it still contributes to $N_{\rm eff}$ by warming up the ν and $\bar{\nu}$ distributions. At $m_\phi = 1\,\text{MeV}$, combining the above bound on y_ν from BBN with that from n-nucleus scattering, yields $Y < 5 \times 10^{-7}$. For $m_\phi > 1\,\text{MeV}$, this bound does not apply because ϕ decays into neutrinos before neutrino decoupling from the plasma. That is why the bound denoted "BBN + n scat." appears as a vertical line in figure 5. Our simplified analysis seems to be in excellent agreement with the results of [50] which solves the full Boltzmann equations.

  ii) LNC case: in this case, the production of scalars via $\nu\nu \to \phi$ is not possible. Processes like $\nu\bar{\nu} \to \nu\bar{\nu}\phi$ or $\nu N \to \nu N \phi$ can take place but are suppressed. The t-channel process $\nu_L \bar{\nu}_L \to \nu_R \bar{\nu}_R$ can lead to ν_R and $\bar{\nu}_R$ production. The $\nu_L \nu_L \to \nu_R \nu_R$ process can also take place but because of cancelation between t and u channel diagrams it has a smaller cross section. The cross section of the dominant production mode is

$$\sigma(\nu_L \bar{\nu}_L \to \nu_R \bar{\nu}_R) = \frac{|y_\nu|^4}{32\pi m_\phi^2} \frac{1}{x^2} \left(\frac{2x(1+x)}{1+2x} - \log(1+2x) \right), \tag{3.6}$$

  where $x = 2E_\nu^2/m_\phi^2$, in which E_ν is the energy of colliding neutrinos in the center-of-mass frame. Taking $n_\nu \sigma H^{-1}|_{T=3\,\text{MeV}} \lesssim 0.3$ ($3\,\text{MeV}$ is the temperature at neutrino decoupling and 0.3 is the bound from CMB on $\delta N_{\rm eff}$ [51]), we find

$$y_\nu < 1.7 \times 10^{-5} \left(\frac{m_\phi^2}{T} \frac{x^2(1+2x)}{2x(1+x) - (1+2x)\log(1+2x)} \right)^{1/4} \Bigg|_{T=3\,\text{MeV}}, \tag{3.7}$$

  in which m_ϕ and T are in MeV and $x = 2T^2/m_\phi^2$. Combining this bound with the one on C_n from neutron-Pb scattering gives the limit denoted "BBN + n scat." in figure 4.

The effective couplings in eq. (2.1) or in eq. (2.2) can lead to contributions at loop level to neutrino mass. Before evaluating the contributions, let us notice that the electroweak symmetric UV-complete models that at low energies give rise to these effective coupling can provide mass for neutrinos at tree level, too. In the models summarized in appendix A, the tree level contribution to neutrino mass turns out to be given by these effective

JHEP05(2018)066

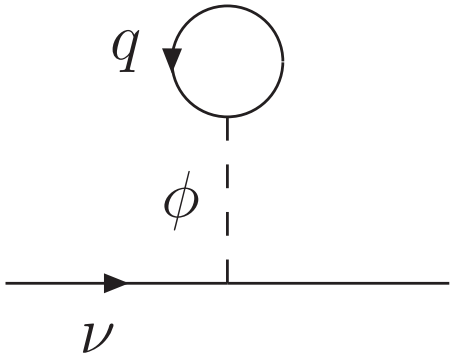

Figure 1. One-loop contribution to neutrino mass.

couplings times the VEV of a new scalar in the model. The VEV can take an arbitrary value to be consistent with the measured neutrino masses. The flavor structure of neutrino mass and y_ν couplings will then have the same pattern. In evaluating the loop contribution from couplings in eqs. (2.1), (2.2) to neutrino mass, one should bear in mind that these couplings are valid only at energies below electroweak scale so the natural UV cutoff is $\Lambda_{\rm cut} \sim 100\,{\rm GeV}$. Neutrino mass term is a helicity-flipping operator so the loop diagram providing neutrino mass has to involve an odd number of helicity flipping y_ν couplings. The direct result of this is that there is no two loop contribution to neutrino mass and at one loop level, the contribution comes from a tadpole contribution to ϕ (as shown in figure 1) which, as usual, can be canceled by a counter-term (see for example sec 11.2 of [52]). At the three loop level, contributions such as the ones in figure 2 arise. In these figures, the lines marked with q and q' denote quarks and the lines without an arrow attached to ϕ lines can denote ν_R (as in case of eq. (2.1)) or ν_L^c (as in case of eq. (2.2)). The contribution from the first diagram can be estimated as

$$m_\nu \sim \frac{(Y^2)^3}{(16\pi^2)^3}\Lambda_{\rm cut} = 10^{-8}{\rm eV}\left(\frac{Y}{8\times10^{-5}}\right)^6\left(\frac{\Lambda_{\rm cut}}{100\,{\rm GeV}}\right)$$

and the other one can be estimated as

$$m_\nu \sim \frac{G_F^2 Y^2}{(16\pi^2)^3}\Lambda_{\rm cut}^5 = 2\times10^{-6}{\rm eV}\left(\frac{Y}{8\times10^{-5}}\right)^2\left(\frac{\Lambda_{\rm cut}}{100\ {\rm GeV}}\right)^5.$$

Both these contributions are too small to be discernible at beta decay experiments or (even in case of LNV coupling) in experiments searching for neutrinoless double beta decay.

Let us now discuss the effects of forward scattering off nuclei due to the new interaction on neutrino propagation in matter composed of nuclei, N. The induced effective mass will be of chirality flipping form as follows

$$\frac{C_N y_\nu}{m_\phi^2}\frac{\rho}{m_N}\left(\nu^T C\nu \quad \text{or} \quad \bar\nu_R\nu_L\right).$$

JHEP05(2018)066

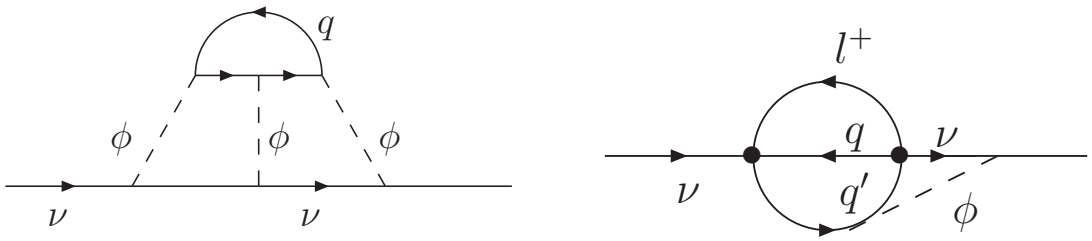

Figure 2. Three loop contributions to neutrino mass. The dots denote charged current weak interaction vertices.

Notice that $m_N \simeq Am_p \simeq Am_n$ and $C_N/m_N \simeq C_p/m_p$ so we can write the effective mass as $(C_p y_\nu/m_\phi^2)(\rho/m_p)$. Taking for example the density of the Sun as $\rho = 150\,\mathrm{g\,cm^{-3}}$, we find a shift in the mass of neutrinos of order of $3\times10^{-12}\,\mathrm{eV}\,(y_\nu/10^{-5})(C_p/10^{-5})(5\ \mathrm{MeV}/m_\phi)^2$, which is completely negligible compared to $\Delta m^2/m_\nu$. One may wonder why forward scattering due to a possible new gauge boson with similar mass and coupling has such a large impact on neutrino propagation in matter, while the present case of a scalar does not. The reason lies in the different Lorentz structure of the induced operators. The vectorial interaction induces a contribution of form $\bar\nu^T\gamma^0\nu = \nu^\dagger\nu$ which has to be compared with m_ν^2/E_ν. In the case of scalar, the matter effects have the operatorial form as the mass themselves and should be compared to the mass splitting, $\Delta m^2/m_\nu$. More detailed discussion can be found in [53].

4 Constraints and future sensitivities from CEνNS

To collect large statistics at coherent scattering energies, CEνNS experiments require intensive and low-energy ($\lesssim 50\,\mathrm{MeV}$) neutrino fluxes. Two types of neutrino sources can be invoked to carry out CEνNS experiments: reactor neutrinos ($E_\nu \lesssim 8\,\mathrm{MeV}$) and pion decay at rest ($E_\nu \lesssim 50\,\mathrm{MeV}$). Two on-going experiments, CONUS [19] and COHERENT [1], adopt these two sources respectively. In this section, we study the sensitivities of the two experiments on light scalar bosons.

4.1 CONUS

The CONUS experiment uses a very low threshold Germanium detector setting 17 m away near a nuclear power plant (3.9 GW thermal power) in Brokdorf, Germany. The total antineutrino flux is $2.5\times10^{13}\,\mathrm{s^{-1}\,cm^{-2}}$. Data collection started in 2017 and first results are expected soon. To study the sensitivity of CONUS, we compute the event numbers given by

$$N_i = \Delta t N_{\mathrm{Ge}} \int_{T_i}^{T_i+\Delta T} dT \int_0^{8\,\mathrm{MeV}} dE_\nu \Phi(E_\nu)\theta\left(T_{\max}(E_\nu) - T\right)\frac{d\sigma}{dT}\left(T,\, E_\nu\right). \tag{4.1}$$

Here Δt is the running time, N_{Ge} is the number of Ge nuclei, $(T_i,\ T_i+\Delta T)$ is the range of recoil energy in each bin, $\Phi(E_\nu)$ is the reactor neutrino flux, and $\theta\left(T_{\max}(E_\nu) - T\right)$ is the Heaviside theta function, equal to 0 for $T_{\max}(E_\nu) - T < 0$ and 1 for $T_{\max}(E_\nu) - T > 0$.

JHEP05(2018)066

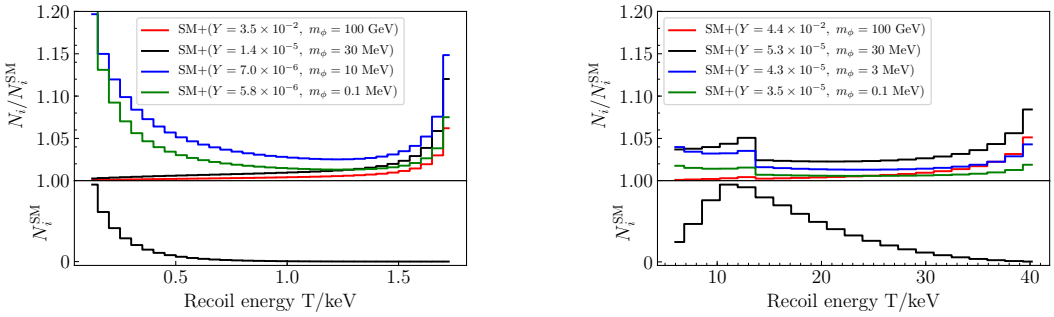

Figure 3. Event excess caused by light scalar bosons in CONUS (left) and COHERENT (right). The effective coupling Y is defined in eq. (2.18) and its dependence on the fundamental quark couplings is given by eq. (2.17). For comparison, the event numbers of the SM signal are also shown.

It is necessary to insert the θ function in (4.1) because the cross section $\frac{d\sigma}{dT}(T, E_\nu)$ does not automatically vanish when $T_{\rm max}(E_\nu) < T$. We take $\Delta t = 1$ year, $\Delta T = 0.05\,\text{keV}$ and $N_{\rm Ge} = 3.32 \times 10^{25}$, corresponding to 4 kg natural Ge (with average atomic number $A = 72.6$). For $\Phi(E_\nu)$, we use a recent theoretical calculation of the flux [54], and normalize it to meet the total antineutrino flux ($2.5 \times 10^{13}\,\text{s}^{-1}\,\text{cm}^{-2}$) in CONUS.

Using eq. (4.1), we compute the event numbers for several examples ($m_\phi = 0.1\,\text{MeV}$, 10 MeV, 30 MeV and 100 GeV) and compare them with the SM value in figure 3. The signal strength is quantified by the ratio N/N_0 where N_0 is the SM expectation, and N contains the additional contributions of light scalar bosons. One can see from the figure that the shape of the spectrum when we include the scalar contribution can be dramatically different, in particular for low values of m_ϕ.

To study the sensitivity of CONUS on light scalar bosons, we adopt the following χ^2-function [13],

$$\chi^2 = \sum_i \frac{[(1+a)N_i - N_i^0]^2}{\sigma_{{\rm stat},i}^2 + \sigma_{{\rm sys},i}^2} + \frac{a^2}{\sigma_a^2}, \tag{4.2}$$

with

$$\sigma_{{\rm stat},i} = \sqrt{N_i + N_{{\rm bkg},i}},\ \sigma_{{\rm sys},i} = \sigma_f (N_i + N_{{\rm bkg},i}). \tag{4.3}$$

The pull parameter a with an uncertainty of $\sigma_a = 2\%$ takes care of the uncertainty in the normalization originating from various sources such as the variation of nuclear fuel supply or the uncertainty of the fiducial mass and distance. Other systematic uncertainties that may change the shape of the event spectrum are parameterized by σ_f in eq. (4.3). Here we assume they are proportional to the event numbers and take $\sigma_f = 1\%$. We also introduce a background in our calculation by adding $N_{{\rm bkg},i}$ to the event number in each bin. The background in CONUS is about 1 count/(day · keV · kg). The threshold of ionization energy detection in CONUS is 0.3 keV, which if divided by the quenching factor (≈ 0.25) corresponds to 1.2 keV recoil energy. The reactor neutrino flux at $E_\nu > 8\,\text{MeV}$ has negligible contributions and also large uncertainties, so we set a cut of E_ν at 8 MeV,

JHEP05(2018)066

$(\sigma_a,\, \sigma_f)$	Y $(m_\phi = 1\,\mathrm{MeV})$	Y $(m_\phi = 5\,\mathrm{MeV})$	Y $(m_\phi = 10\,\mathrm{MeV})$	Y $(m_\phi = 30\,\mathrm{MeV})$
(0.5%, 0.1%)	2.0×10^{-6}	3.3×10^{-6}	6.4×10^{-6}	11.8×10^{-6}
(0.6%, 0.3%)	2.5×10^{-6}	3.9×10^{-6}	7.0×10^{-6}	13.3×10^{-6}
(1.0%, 0.5%)	2.8×10^{-6}	4.4×10^{-6}	7.9×10^{-6}	14.5×10^{-6}
(2.0%, 1.0%)	3.3×10^{-6}	5.1×10^{-6}	9.5×10^{-6}	16.7×10^{-6}

Table 1. Uncertainties of the reactor neutrino flux assumed in CONUS100 and the corresponding bounds on Y.

which corresponds to about 1.75 keV recoil energy according to eq. (2.7). As a result, in eq. (4.2) we only sum over the bins from 1.2 keV to 1.75 keV.

The result is shown in figure 4 and figure 5 for the LNC and LNV cases respectively. Although the constraints of CEνNS experiments are independent of the LNC/LNV cases, the other constraints depend on the nature of the interaction, as explained in section 3. We therefore present the two cases separately.

We also study future improved sensitivities of CONUS by assuming a 100 kg Germanium detector as the target and an improved threshold down to 0.1 keV. We assume the corresponding systematic uncertainties are also reduced to a matching level, $(\sigma_a, \sigma_f) = (0.5\%, 0.1\%)$. This will be possible if the reactor neutrino flux is better understood due to improved theoretical models and measurements. The forecast for CONUS100 with 5 years of data taking is also shown in figures 4, 5 with blue dashed lines. If the flux uncertainties can not be reduced to such an optimistic level, then the constraint should be between the upcoming bound (blue solid curve) and the optimistic bound (blue dashed curve). In table 1, we assume several different flux uncertainties and compute the corresponding bounds on Y. Since we care about to what extent the CONUS bound could be improved in the future, we prefer to present in figure 4 and figure 5 the most optimistic bounds together with the upcoming (realistic) bounds so that other possibilities fall into the gap between them.

As mentioned above, the shape information for light scalar masses is noteworthy in the spectrum, see eq. (2.8). It can in fact be used to determine the value of the mass. In figure 6 we show the potential of CONUS100 for determining the mass and coupling of the ϕ particle assuming two characteristic examples. As long as the mass of the scalar is not much larger than the neutrino energy or the typical momentum exchange, $m_\phi^2 \sim MT \sim E_\nu^2$, reconstruction of the mass is possible.

4.2 COHERENT

The COHERENT experiment uses a CsI scintillator to detect neutrinos produced by π^+ and μ^+ decay at rest. In its recent groundbreaking publication [1] a 6.7σ observation of the SM coherent scattering was announced. There are three types of neutrinos in the neutrino flux, ν_μ, $\overline{\nu}_\mu$, and ν_e. The first is produced in the decay $\pi^+ \to \mu^+ + \nu_\mu$ while the second and the third are produced in the subsequent decay $\mu^+ \to e^+ + \overline{\nu}_\mu + \nu_e$. Because the first decay is a two-body decay and the pion is at rest, the produced neutrinos will be monochromatic

JHEP05(2018)066

with energy:

$$E_{\nu 0} = \frac{m_\pi^2 - m_\mu^2}{2m_\pi} \approx 29.8 \text{ MeV},$$

where $m_\mu = 105.66\,\text{MeV}$ and $m_\pi = 139.57\,\text{MeV}$ are the muon and pion masses, respectively. Remembering that the muon also decays at rest, the neutrino fluxes are given by [55]:

$$\phi_{\nu_\mu}(E_\nu) = \phi_0 \delta\left(E_\nu - E_{\nu 0}\right), \tag{4.4}$$

$$\phi_{\overline{\nu}_\mu}(E_\nu) = \phi_0 \frac{64 E_\nu^2}{m_\mu^3}\left(\frac{3}{4} - \frac{E_\nu}{m_\mu}\right), \tag{4.5}$$

$$\phi_{\nu_e} = \phi_0 \frac{192 E_\nu^2}{m_\mu^3}\left(\frac{1}{2} - \frac{E_\nu}{m_\mu}\right), \tag{4.6}$$

where E_ν should be in the range $(0,\, m_\mu/2)$. The event numbers are computed by

$$N_i = \Delta t N_{\text{Cs/I}} \int_{T_i}^{T_i+\Delta T} dT \left[\phi_0 \theta\left(T,\, T_{\max}(E_{\nu 0})\right) \frac{d\sigma}{dT}\left(T,\, E_{\nu 0}\right) + \int_0^{m_\mu/2} dE_\nu \left(\phi_{\overline{\nu}_\mu}(E_\nu) + \phi_{\nu_e}(E_\nu)\right) \theta\left(T,\, T_{\max}(E_\nu)\right) \frac{d\sigma}{dT}\left(T,\, E_\nu\right)\right], \tag{4.7}$$

which is similar to eq. (4.1) except that (i) N_{Ge} is replaced with $N_{\text{Cs/I}}$; (ii) for the ν_μ flux, the delta function in eq. (4.4) has been integrated out. For simplicity, we assume that Cs and I have approximately the same proton and neutron numbers, $(Z,\, A) = (54,\, 130)$. We also assume that the couplings of neutrinos are flavor universal ($(y_\nu)_{\alpha\beta} = y_\nu$), so we take equal cross section for all neutrino flavors. Using eq. (4.7), we also compute the ratio N/N_0 in COHERENT, shown in the right panel of figure 3. Note that there is a kink around 14 keV in the event spectrum. This is caused by the monochromatic ν_μ beam with $E_\nu = 29.8\,\text{MeV}$, which corresponds to the maximal recoil energy $T \approx 2E_\nu^2/M \approx 13.7$ keV. Therefore, the monochromatic ν_μ beam generates events with $T \leq 13.7$ keV but does not contribute to signals with higher recoil energies. Consequently, a kink appears in figure 3 around 14 keV.

In the COHERENT experiment, the recoil energy of the nucleus is converted to multiple photoelectrons and eventually detected by PMTs. The number of photoelectrons n_{PE} is approximately proportional to the recoil energy [1]:

$$n_{\text{PE}} \approx 1.17 \frac{T}{\text{keV}}. \tag{4.8}$$

For $n_{\text{PE}} > 20$, the signal acceptance fraction is about 70% (cf. figure S9 of [1]). This number drops down quickly for smaller n_{PE}, and becomes approximately zero for $n_{\text{PE}} < 5$. This implies that the threshold for T is about 4 keV in COHERENT. Using eqs. (4.7), (4.8) and the signal acceptance fraction data, we can study the constraint of the COHERENT data (from figure 3 of [1]) on light scalar bosons. The SM expectation is also provided by [1] which can be used to compute the total normalization factor. We directly use the relevant uncertainties provided by [1]. The result is shown in figures 4 and 5 as well. Since reactor neutrinos

JHEP05(2018)066

provide much larger event numbers, CONUS limits will be better, though of course limited to the electron-type couplings, whereas COHERENT will also have muon-type neutrinos.

In the future, the COHERENT experiment will further develop the detection of CEνNS with different targets,[4] including 30 kg liquid argon, 10 kg high purity Ge, and 185 kg NaI crystal. A complete study on the future sensitivities of future COHERENT including all the different targets and different detection technology is beyond the scope of this paper. Considering that the total fiducial mass compared to the current value (14.6 kg CsI) will be increased by a factor of ~ 20, plus a prolonged running for few years, at best the statistics may be increased by a factor of 100, which corresponds to a reduction of the statistical uncertainties by a factor of 10. It is therefore reasonable to assume that the uncertainties of future measurement will be reduced by a factor between 1 and 10. To show the sensitivity of future COHERENT versions on the light scalar coupling, we plot a black dashed curve in figure 4 and figure 5 assuming the uncertainties (both systematical and statistical) are reduced by a factor of 10. For the sake of definiteness, we take the liberty to denote this potential situation as COHERENT (stat. $\times$ 100). Again, the determination of the mass of the scalar particle is possible if its mass lies below the typical neutrino energy. As seen in figure 3, the spectral distortion due to the scalar exchange is less dramatic as for CONUS. This is mostly caused by the larger energy of the neutrinos, the momentum exchange and nuclear recoil. Figure 6 shows the potential of the assumed future COHERENT version for determining the mass and coupling of the ϕ particle, assuming two characteristic examples. Due to the larger energy of COHERENT, and also because of the smaller statistics, the reconstruction potential is less promising compared to experiments based on reactor neutrinos.

5 Interpretation of the results

Figures 4 and 5 show the constraints and limits on the relevant combination of Y couplings versus the mass of the scalar for lepton number conserving and lepton number violating interactions, respectively. To draw these lines the coupling of ϕ to neutrinos is taken to be flavor universal. Each limit is however sensitive to a different flavor structure. Let us start by discussing the bounds which apply for both lepton number violating and lepton number conserving interactions. The red-dashed lines show the constraint on $Y \simeq \sqrt{y_\nu C_n}$ from combining the upper bounds on C_n and y_ν from the n-Pb scattering and meson decay experiments. As seen from the figures, this bound is relatively weak. The present bound from COHERENT shown by a solid black line is already well below this combined bound. The bounds from meson decay are sensitive to $\sum_\alpha (y_\nu)^2_{e\alpha}$ and $\sum_\alpha (y_\nu)^2_{\mu\alpha}$. Since the beam at the COHERENT experiment is composed of ν_μ $\bar{\nu}_\mu$ and ν_e fluxes, it will be sensitive to similar flavor composition. Our forecast for the future bound by the COHERENT experiment (a factor 10 smaller uncertainties) is shown by dashed black line; the bound on Y can be improved by a factor of 2. The blue solid and dashed lines are the upper bounds that CONUS can set with 1 year $\times$ 4 kg and 5 year $\times$ 100 kg of data taking, respectively. As seen from these figures, CONUS can improve the bound by one or two

[4] See: http://webhome.phy.duke.edu/~schol/COHERENT_Yue.pdf.

JHEP05(2018)066

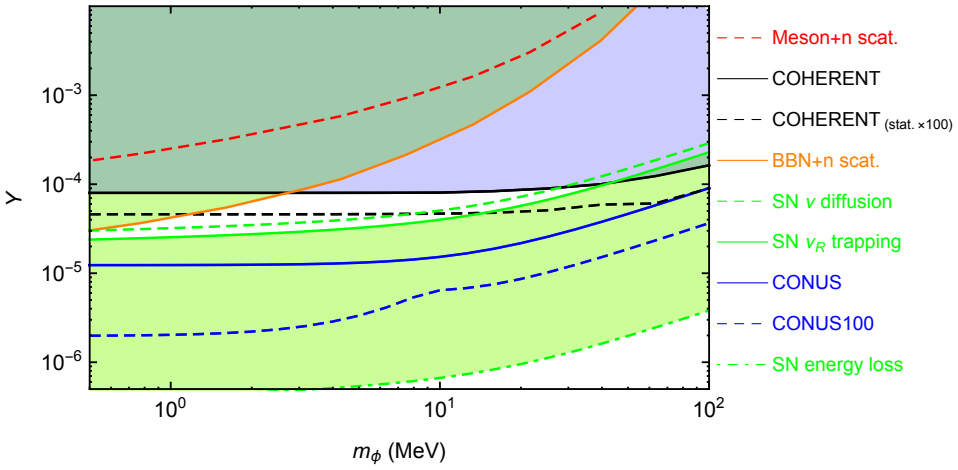

Figure 4. Constraints from CEνNS experiments on (Y, m_ϕ) for a lepton number conserving interaction, see eq. (2.1). The black, dashed black, blue, and dashed blue curves correspond to the 95% C.L. constraint of the recent COHERENT data, the sensitivities of future COHERENT, CONUS 4 kg×1 year, and CONUS 100 kg×5 years (light-blue) respectively. Various other limits from particle and astroparticle physics are explained in section 3.

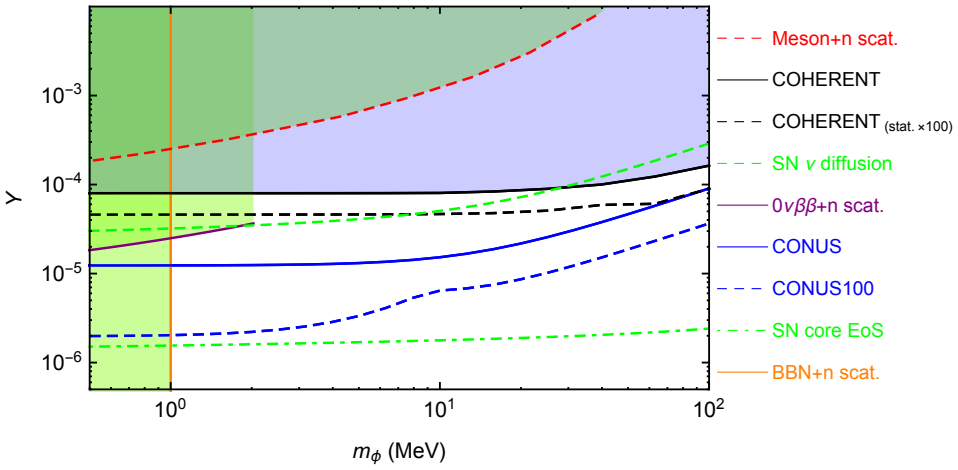

Figure 5. Similar to figure 4 but for lepton number violating interactions, see eq. (2.2).

JHEP05(2018)066

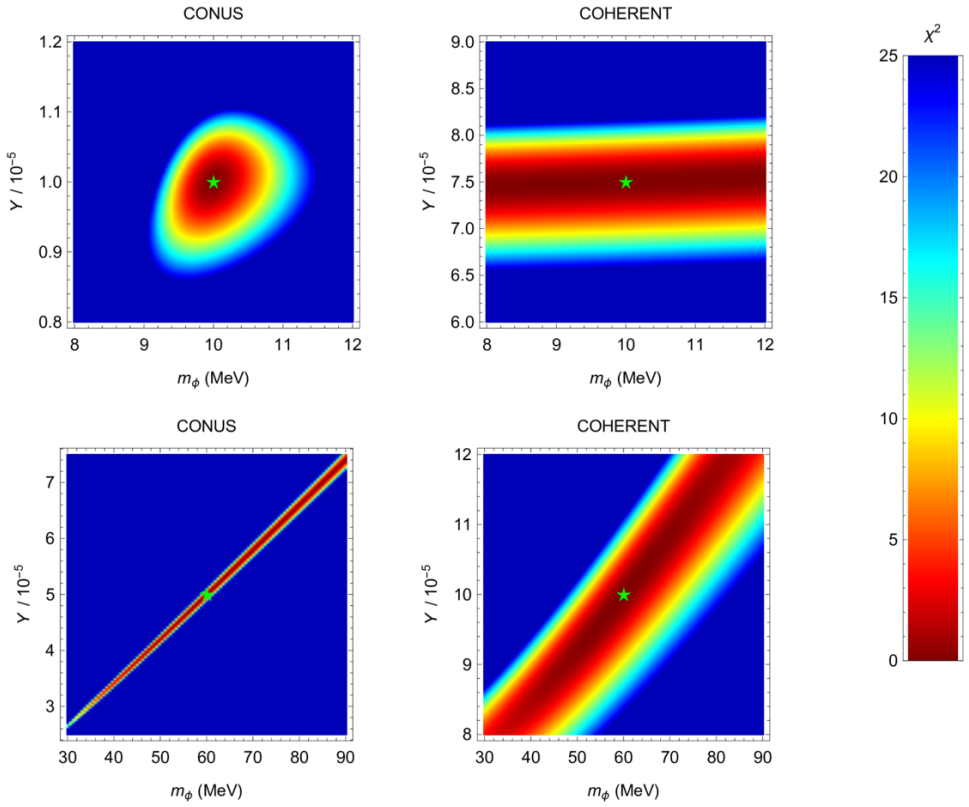

Figure 6. Measurements of the mass m_ϕ and coupling Y in CONUS100 (left panels) and COHERENT (stat. $\times$ 100) (right panels) assuming the presence of a scalar boson, with the true values indicated by the green stars.

orders of magnitudes. Since CONUS is a reactor neutrino experiment, it can only probe $C_n^{1/2}(\sum_\alpha |y_\nu|^2_{e\alpha})^{1/4}$. Since the uncertainties of CONUS are mainly limited by statistics, the bound that it can set on the cross section σ_ϕ scales as $t^{-1/2}$ with data taking time. Since $\sigma_\phi \propto Y^4$, the bound on Y will scale as $t^{-1/8}$.

The violet curve in figure 5 up to 2.4 MeV is the combined bound from the n-Pb scattering on C_n and from double beta decay on $(y_\nu)_{ee}$. CONUS with only one year of data taking can provide a stronger bound. The dashed green lines in figures 4 and 5 denoted "SN ν diffusion" show the limits resulting essentially from a neutrino-nucleon scattering cross section due to ϕ exchange being equal to that in the SM. As we discussed before, in the vicinity of this line supernova evolution and emitted neutrino flux will be dramatically affected. As seen from the figures, the CONUS experiment with 1 year of data taking can already probe all this range. The green area between solid and dotted-dashed green lines in figure 5 is ruled out by supernova cooling and ν_R trapping considerations.

In the LNC case, the orange line in figure 4 denoted by "BBN + n scat." shows the combined bound from n-Pb scattering and BBN. As seen from the figure, for $m_\phi > 3$ MeV,

JHEP05(2018)066

the bound from COHERENT is already stronger. Both for LNC and LNV cases, a ϕ particle with $m_\phi \in (1.5-3)\,\text{MeV}$ and $y_\nu \sim \text{few} \times 10^{-5}$ can significantly affect BBN. As seen from the figures this mass range can be probed by CEνNS experiments. For $\sqrt{C_n|y_\nu|_{e\alpha}}$ above the dotted-dashed green line in figure 5, the equation of state in supernova inner core will drastically change because of $\nu_e + n \to \bar{\nu}_\alpha + n$ scattering. As seen from the figure, a significant part of the parameter space above this line can be probed by CONUS. We can therefore deduce that coherent scattering results may have dramatic impact on SN and BBN physics.

Figure 6 displays the prospect of measuring m_ϕ and Y by our future versions of CONUS and COHERENT, assuming true values of $(m_\phi,\ Y)$ are $(10\ \text{MeV},\ 10^{-5})$ or $(60\ \text{MeV},\ 5\times 10^{-5})$ for CONUS100, and $(10\ \text{MeV},\ 7.5\times 10^{-5})$ or $(60\ \text{MeV},\ 10^{-4})$ for COHERENT (stat. $\times$ 100). Here for comparison, we choose the same masses for the two experiments. However, the couplings in COHERENT (stat. $\times$ 100) are set to larger values to lead to similar precision as CONUS100 (cf. figures 4 and 5). Even with larger couplings, COHERENT still cannot measure $(m_\phi,\ Y)$ as good as CONUS100. As shown in figure 6, for true values $m_\phi = 10\,\text{MeV}$ and $Y = 10^{-5}$, the mass and coupling can be determined with better than 10% accuracy by CONUS100. In comparison, COHERENT (stat. $\times$ 100) loses its capability to determine m_ϕ but it has still reasonable precision in determining Y provided that Y is large enough (close to its present bound). This is understandable because $m_\phi = 10\,\text{MeV}$ is larger than the typical energy-momentum transfer in the CONUS100 ($m_\phi^2 \gtrsim MT \sim E_\nu^2$) but is smaller than the energy-momentum transfer in COHERENT ($m_\phi^2 \lesssim MT \sim E_\nu^2$). Another reason is the better statistics in CONUS. If the mass is raised to 60 MeV, then both lose their ability to determine the mass and the coupling separately. They however maintain their sensitivity to Y/m_ϕ. In principle, there could be a scenario where the future COHERENT experiment is able to determine the mass. For example, as we have checked, if $(Y,\ m_\phi) = (10^{-4},\ 10\ \text{MeV})$, then the coupling and the mass can be determined separately by the future COHERENT experiment. However, such a large coupling has already been excluded by the current COHERENT data. To find a scenario which is not excluded by the current COHERENT data but still within the sensitivity of future COHERENT, we can only choose $(Y,\ m_\phi)$ in the band between the black solid and dashed curves in figure 4. Since the band is too narrow, we cannot find such a scenario where the mass can be determined. Besides, the difference between s-channel and t-channel signals is also a reason. The new scalar boson causes a t-channel process. In the s-channel, it is crucial to have the energy match the new boson mass to get the resonance, which provides useful information on the mass and the coupling. For example, the masses of the Z boson or Higgs can be precisely measured from the resonances observed in colliders. The measurement of masses in the t-channel, however, depends rather on the high statistics and low thresholds, which is the strength of CONUS.

Discovering a positive signal for the effects of ϕ by CONUS will have drastic consequences for the analysis of supernova evolution. If a value of Y below the green solid line in figure 4 is found, the supernova cooling bounds tell us that interaction cannot involve ν_R so the interaction should be of lepton number violating form. If ϕ turns out to have a mass around 2 MeV, it will be more intriguing as it may be discovered at double beta experiments. If, however, double beta decay searches fail to discover ϕ with expected mass and

JHEP05(2018)066

coupling, we may draw a conclusion that $(y_\nu)_{ee} \ll (y_\nu)_{e\mu}, (y_\nu)_{e\tau}$. In any case, in analyzing BBN, effects of such light m_ϕ with sizeable Y has to be taken into account. Comparing figures 4 and 5, we conclude that because of the BBN bounds, discovery of $m_\phi < 1\,\text{MeV}$ will indicate LNC interaction with light right-handed neutrinos with immediate consequences for supernova evolution.

If CONUS and/or COHERENT finds $Y \sim 10^{-5}$, the chances of finding a signal for ϕ in meson decay experiments as well as in n-Pb scattering experiments increase. If CONUS finds a signal for $Y > 5 \times 10^{-5}$, this means that signals for $K^+ \to e^+\nu\phi$ and for $\pi^+ \to e^+\nu\phi$ will be within reach of next generation [56], and new n-Pb measurements would be very interesting. If CONUS finds $Y < 10^{-5}$ and if meson decay experiments find $y_\nu \gtrsim 10^{-4}$, we would conclude $C_n < 10^{-6}$, making it difficult to see an effect on n-Pb scattering experiments. Similarly $Y < 10^{-5}$ and $C_n \sim 10^{-4}$ (close to the present bound) would imply $y_\nu < 10^{-6}$.

We conclude this section by mentioning some possibilities on inferring the flavor structure or type of interaction that arise due to the complementarity of the various sources and limits. If the ν_e couplings are large enough to be within the reach of COHERENT (that is if $Y > 5 \times 10^{-5}$), the CONUS experiment will easily determine $\sum_\alpha |(y_\nu)_{e\alpha}|^2 C_N^2$, where α runs over all active flavors for the LNV case (over all light right-handed species for LNC case). The information by COHERENT can then determine $\sum_\alpha |(y_\nu)_{\mu\alpha}|^2 C_N^2$. If COHERENT alone would be able to distinguish the flavor content of the events (e.g. by timing cuts), information on flavor structure of y_ν (i.e. on $\sum_\alpha |(y_\nu)_{\mu\alpha}|^2 / \sum_\alpha |(y_\nu)_{e\alpha}|^2$) could be extracted. In the special case that $|(y_\nu)_{e\alpha}| \ll |(y_\nu)_{\mu\alpha}|$, it may be possible that COHERENT will discover new effect but CONUS will report null results for new physics discovery.

6 Summary and concluding remarks

Coherent elastic neutrino-nucleus scattering can probe both new light as well as heavy physics. Focussing here on the light case we demonstrated the discovery potential of current and future coherent scattering experiments on the mass and coupling of scalar particles interacting with neutrinos and quarks. The shape of the nuclear recoil spectrum is distorted by the scalar interaction, and allows even to determine the mass of the scalar, if its mass is around the energy of the scattered neutrinos. Even current limits by COHERENT are competitive with a combination of bounds from BBN and from various terrestrial experiments such as meson decay and neutron-scattering experiments. Moreover, these bounds probe areas in parameter space that can have important consequences for BBN and supernova evolution, in particular for lepton number violating interactions. Future versions of the experiment or upcoming reactor experiments such as CONUS will reach not yet explored areas in parameter space.

Acknowledgments

We thank Giorgio Arcadi, Tommy Ohlsson, Kate Scholberg and Stefan Vogl for many helpful discussions. YF thanks MPIK Heidelberg where a part of this work was done for their

JHEP05(2018)066

hospitality. This project has received funding from the European Union's Horizon 2020 research and innovation programme under the Marie Sklodowska-Curie grant agreement No 674896 and No 690575. YF is also grateful to ICTP associate office for partial financial support. WR is supported by the DFG with grant RO 2516/6-1 in the Heisenberg program.

A Suggestions for underlying electroweak symmetric models

In this section we show how one can build a toy model symmetric under $\mathrm{SU}(2)\times\mathrm{U}(1)$ that can give rise to effective coupling of form

$$\bar{q}\Gamma_q q\phi \equiv \bar{q}(C_q + i\gamma^5 D_q)q\phi$$

as well as the ones shown in eqs. (2.1), (2.2). The coupling of ϕ to nuclei should of course arise from its coupling to quarks. The latter can originate from the mixing of the singlet scalar ϕ with an electroweak doublet, Φ. Taking complex couplings of form

$$Y_u \bar{u}_R \Phi^T C Q + \text{H.c. and } Y_d \bar{d}_R \Phi^\dagger Q + \text{H.c.} \tag{A.1}$$

and a mixing of β between ϕ and the neutral component of Φ, we find the coupling of ϕ to the u and d quarks respectively to be given by $\Gamma_u = \sin\beta\, Y_u^*$ and $\Gamma_d = \sin\beta Y_d^*$, or equivalently

$$C_q = \mathcal{R}[Y_q]\sin\beta \quad \text{and} \quad D_q = \mathcal{I}[Y_q]\sin\beta. \tag{A.2}$$

Notice that taking Y_q to be real, the coupling will be parity invariant and therefore $D_q = 0$.

The most economic solution is to identify Φ with the SM Higgs. Remember that the couplings of the SM Higgs to quarks of first generation are $\mathcal{O}(10^{-5})$. Moreover, the mixing of ϕ with SM Higgs cannot exceed $\mathcal{O}(10^{-2})$, otherwise the rate of invisible decay mode $Br(H\to\phi\phi)$ will exceed the experimental limits. Combining these, we conclude that in case ϕ is taken to be the SM Higgs, $|\Gamma_{q\phi}| \sim 10^{-2}\, m_q/\langle H^0\rangle$. As we have seen in section 2.3, the contributions from quarks of different generations to the coupling of a nucleus to ϕ will be of the same order and too small to lead to discernable effects on current CEνNS experiments.

Taking thus Φ to be a new doublet, its coupling to quarks can in principle be as large as $\mathcal{O}(1)$. Taking

$$V(\phi,\Phi) = \frac{m_1^2}{2}\phi^2 + m_2^2|\Phi|^2 + (A\phi H^\dagger\cdot\Phi + \text{H.c.}),$$

we obtain $\sin\beta = A\langle H\rangle/(m_2^2 - m_1^2)$, $m_\Phi \simeq m_2$ and $m_\phi \simeq \sqrt{m_1^2 - m_\Phi^2\sin^2\beta}$. To avoid a need for fine-tuned cancelation $m_\Phi\sin\beta$ should be smaller than $\mathcal{O}(m_\phi)$. For $m_\phi\sim 5\,\mathrm{MeV}$ and $m_\Phi\sim 1\,\mathrm{TeV}$, this implies $\sin\beta\sim 10^{-5}$. For $\Gamma_u\sim\Gamma_d\sim 10^{-5}$, naturalness (i.e., absence of fine-tuned cancelation) requires the mass of Φ to be within the reach of the LHC and its coupling to u and d quarks to be $\mathcal{O}(1)$ which in turn promises a rich phenomenology at the LHC.

In what regards neutrinos,[5] considering first the LNC interaction, a mechanism similar to the one described above can provide a lepton number conserving interaction of $\phi\bar{\nu}_R\nu_L$ through mixing of ϕ with neutral component of the Φ doublet. For a lepton number violating coupling $\phi\nu^T C\nu$, two scenarios can be realized:

[5] A model in which a scalar couples both to neutrinos and charged leptons has been considered in [57].

JHEP05(2018)066

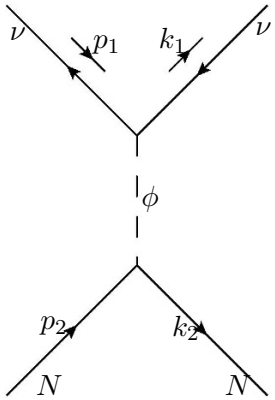

Figure 7. The Feynman diagram of coherent $\overline{\nu}N$ scattering mediated by the new light scalar boson.

- The $\phi\nu^T C\nu$ coupling can be obtained by the mixing of ϕ with a neutral component of an electroweak triplet Δ which couples to the left-handed lepton doublet as $L^T C\Delta L$. The quantum numbers of Δ should be the same as the triplet scalar whose tiny vacuum expectation value is responsible for neutrino mass in the type II seesaw mechanism. Identifying these two, the flavor structure of the ϕ coupling to neutrinos will be determined by that of neutrino mass: $(C_\nu)_{\alpha\beta}, (D_\nu)_{\alpha\beta} \propto (m_\nu)_{\alpha\beta}$. Naturalness (i.e., $m_\phi \sim 1$ MeV $\ll m_\Delta \sim$ TeV without fine tuned cancelation) again implies that Δ is not much heavier than TeV and its coupling to leptons are of order of 1 which promises rich phenomenology at the LHC such as production of Δ^{++} and its decay into a same sign pair of charged leptons.

- Another scenario that can provide coupling of form $\phi\nu^T C\nu$ is suggested in [58]. The scenario is very similar to the inverse seesaw mechanism for generating mass for neutrinos and requires a Dirac fermion singlet Ψ with the following Lagrangian

$$\mathcal{L} = M_\Psi \bar{\Psi}\Psi + y\bar{\Psi}_R H^T C L + y'\phi\Psi_R^T C\Psi_R. \tag{A.3}$$

  When $M_\Psi \gg m_\phi$, we can integrate out Ψ and arrive at $C_\nu = (y\langle H\rangle/M_\Psi)^2 y'$. As shown in [58], C_ν even as large as 10^{-3} can be obtained by this mechanism. Moreover, if ϕ develops a vacuum expectation value, an inverse seesaw mechanism for neutrino mass generation will emerge and the flavor structure of C_ν and neutrino mass matrix will be similar. In this scenario, the SM Higgs will have an invisible decay mode $H \to \bar{\Psi}\nu_L$ governed by y^2.

The discovery of a scalar field in coherent scattering experiments will therefore, at least in the models outlined here, hint towards rich new collider phenomenology.

B Calculation of the cross section

In this appendix, we give the analytic calculation of $\overline{\nu}N$ and νN cross sections, assuming a lepton number conserving interaction with ϕ. The cross section for the lepton number

JHEP05(2018)066

violating case is identical. Let us first focus on the $\overline{\nu}N$ case. The initial and final momenta are denoted in the way shown in figure 7. The scattering amplitude of this diagram is

$$i\mathcal{M}_\phi = \overline{v}^s(p_1)P_R\,(i\Gamma_{\nu\phi})\,v^{s'}(k_1)\frac{-i}{q^2-m_\phi^2}\overline{u}^{r'}(k_2)\,(i\Gamma_{N\phi})\,u^r(p_2), \tag{B.1}$$

where $\Gamma_{\nu\phi} \equiv C_\nu + D_\nu i\gamma^5$ and

$$q = p_1 - k_1,\ q^2 = -2MT. \tag{B.2}$$

We have inserted a right-handed projector $P_R = (1+\gamma^5)/2$ in eq. (B.1) because the initial antineutrino produced by the charged current interaction should be right-handed. Because of P_R, if the initial antineutrino is left-handed, the amplitude automatically vanishes. We can therefore sum over all the spins and apply the trace technology:

$$\begin{aligned}|i\mathcal{M}_\phi|^2 &= \frac{1}{(2MT+m_\phi^2)^2}\mathrm{tr}\left[\gamma\cdot p_1 P_R\Gamma_{\nu\phi}\gamma\cdot k_1\Gamma_{\nu\phi}P_L\right] \\ &\quad\times\frac{1}{2}\mathrm{tr}\left[(\gamma\cdot k_2+M)\Gamma_{N\phi}(\gamma\cdot p_2+M)\Gamma_{N\phi}\right]. \qquad \text{(B.3)}\\ &= \frac{1}{(2MT+m_\phi^2)^2}\mathrm{tr}\left[\gamma\cdot p_1 P_R\gamma\cdot k_1(C_\nu^2+D_\nu^2)P_L\right]2M\left[C_N^2(2M+T)+D_N^2T\right]. \qquad \text{(B.4)}\end{aligned}$$

For νN scattering, one needs to change eq. (B.1) to

$$i\mathcal{M}_\phi = \overline{u}^s(p_1)P_L\,(i\Gamma_{\nu\phi})\,u^{s'}(k_1)\frac{-i}{q^2-m_\phi^2}\overline{u}^{r'}(k_2)\,(i\Gamma_{N\phi})\,u^r(p_2). \tag{B.5}$$

Consequently, one has to interchange $P_R \leftrightarrow P_L$ in eq. (B.3). From eq. (B.4) we can see that $P_R \leftrightarrow P_L$ does not change the result so the cross sections are equal for $\overline{\nu}N$ and νN scattering. From eq. (B.4) we obtain

$$\frac{d\sigma_\phi}{dT} = \frac{M|y_\nu|^2}{4\pi(2MT+m_\phi^2)^2}\left[C_N^2\frac{MT}{E_\nu^2} + \left(C_N^2+D_N^2\right)\frac{T^2}{2E_\nu^2}\right], \tag{B.6}$$

which is the cross section for both neutrino and antineutrino scattering.

Open Access. This article is distributed under the terms of the Creative Commons Attribution License (CC-BY 4.0), which permits any use, distribution and reproduction in any medium, provided the original author(s) and source are credited.

References

[1] COHERENT collaboration, D. Akimov et al., *Observation of coherent elastic neutrino-nucleus scattering*, *Science* **357** (2017) 1123 [arXiv:1708.01294] [INSPIRE].

[2] K. Scholberg, *Prospects for measuring coherent neutrino-nucleus elastic scattering at a stopped-pion neutrino source*, *Phys. Rev.* **D 73** (2006) 033005 [hep-ex/0511042] [INSPIRE].

[3] M. Cadeddu, C. Giunti, Y.F. Li and Y.Y. Zhang, *Average CsI neutron density distribution from COHERENT data*, *Phys. Rev. Lett.* **120** (2018) 072501 [arXiv:1710.02730] [INSPIRE].

JHEP05(2018)066

[4] A.C. Dodd, E. Papageorgiu and S. Ranfone, *The effect of a neutrino magnetic moment on nuclear excitation processes*, *Phys. Lett.* **B 266** (1991) 434 [INSPIRE].

[5] T.S. Kosmas, O.G. Miranda, D.K. Papoulias, M. Tortola and J.W.F. Valle, *Probing neutrino magnetic moments at the Spallation Neutron Source facility*, *Phys. Rev.* **D 92** (2015) 013011 [arXiv:1505.03202] [INSPIRE].

[6] A.J. Anderson et al., *Measuring active-to-sterile neutrino oscillations with neutral current coherent neutrino-nucleus scattering*, *Phys. Rev.* **D 86** (2012) 013004 [arXiv:1201.3805] [INSPIRE].

[7] B. Dutta, Y. Gao, R. Mahapatra, N. Mirabolfathi, L.E. Strigari and J.W. Walker, *Sensitivity to oscillation with a sterile fourth generation neutrino from ultra-low threshold neutrino-nucleus coherent scattering*, *Phys. Rev.* **D 94** (2016) 093002 [arXiv:1511.02834] [INSPIRE].

[8] B.C. Cañas, E.A. Garcés, O.G. Miranda and A. Parada, *The reactor antineutrino anomaly and low energy threshold neutrino experiments*, *Phys. Lett.* **B 776** (2018) 451 [arXiv:1708.09518] [INSPIRE].

[9] T.S. Kosmas, D.K. Papoulias, M. Tortola and J.W.F. Valle, *Probing light sterile neutrino signatures at reactor and Spallation Neutron Source neutrino experiments*, *Phys. Rev.* **D 96** (2017) 063013 [arXiv:1703.00054] [INSPIRE].

[10] J. Barranco, O.G. Miranda and T.I. Rashba, *Probing new physics with coherent neutrino scattering off nuclei*, *JHEP* **12** (2005) 021 [hep-ph/0508299] [INSPIRE].

[11] J. Barranco, O.G. Miranda and T.I. Rashba, *Low energy neutrino experiments sensitivity to physics beyond the Standard Model*, *Phys. Rev.* **D 76** (2007) 073008 [hep-ph/0702175] [INSPIRE].

[12] B. Dutta, R. Mahapatra, L.E. Strigari and J.W. Walker, *Sensitivity to Z-prime and nonstandard neutrino interactions from ultralow threshold neutrino-nucleus coherent scattering*, *Phys. Rev.* **D 93** (2016) 013015 [arXiv:1508.07981] [INSPIRE].

[13] M. Lindner, W. Rodejohann and X.-J. Xu, *Coherent neutrino-nucleus scattering and new neutrino interactions*, *JHEP* **03** (2017) 097 [arXiv:1612.04150] [INSPIRE].

[14] I.M. Shoemaker, *COHERENT search strategy for beyond Standard Model neutrino interactions*, *Phys. Rev.* **D 95** (2017) 115028 [arXiv:1703.05774] [INSPIRE].

[15] J. Liao and D. Marfatia, *COHERENT constraints on nonstandard neutrino interactions*, *Phys. Lett.* **B 775** (2017) 54 [arXiv:1708.04255] [INSPIRE].

[16] P. Coloma, M.C. Gonzalez-Garcia, M. Maltoni and T. Schwetz, *COHERENT enlightenment of the neutrino dark side*, *Phys. Rev.* **D 96** (2017) 115007 [arXiv:1708.02899] [INSPIRE].

[17] J.B. Dent, B. Dutta, S. Liao, J.L. Newstead, L.E. Strigari and J.W. Walker, *Accelerator and reactor complementarity in coherent neutrino-nucleus scattering*, *Phys. Rev.* **D 97** (2018) 035009 [arXiv:1711.03521] [INSPIRE].

[18] D.K. Papoulias and T.S. Kosmas, *COHERENT constraints to conventional and exotic neutrino physics*, *Phys. Rev.* **D 97** (2018) 033003 [arXiv:1711.09773] [INSPIRE].

[19] C. Buck et al., *The CONUS experiment — COherent elastic NeUtrino nucleus Scattering*, https://indico.cern.ch/event/606690/contributions/2591545/attachments/1499330/2336272/Taup2017_CONUS_talk_JHakenmueller.pdf.

JHEP05(2018)066

[20] H.T. Wong, *Neutrino-nucleus coherent scattering and dark matter searches with sub-keV germanium detector*, *Nucl. Phys.* **A 844** (2010) 229C [INSPIRE].

[21] CONNIE collaboration, A. Aguilar-Arevalo et al., *The CONNIE experiment*, *J. Phys. Conf. Ser.* **761** (2016) 012057 [arXiv:1608.01565] [INSPIRE].

[22] MINER collaboration, G. Agnolet et al., *Background studies for the MINER coherent neutrino scattering reactor experiment*, *Nucl. Instrum. Meth.* **A 853** (2017) 53 [arXiv:1609.02066] [INSPIRE].

[23] V. Belov et al., *The νGeN experiment at the Kalinin nuclear power plant*, 2015 *JINST* **10** P12011 [INSPIRE].

[24] J. Billard et al., *Coherent neutrino scattering with low temperature bolometers at CHOOZ reactor complex*, *J. Phys.* **G 44** (2017) 105101 [arXiv:1612.09035] [INSPIRE].

[25] R. Strauss et al., *The ν-cleus experiment: a gram-scale fiducial-volume cryogenic detector for the first detection of coherent neutrino-nucleus scattering*, *Eur. Phys. J.* **C 77** (2017) 506 [arXiv:1704.04320] [INSPIRE].

[26] J.B. Dent, B. Dutta, S. Liao, J.L. Newstead, L.E. Strigari and J.W. Walker, *Probing light mediators at ultralow threshold energies with coherent elastic neutrino-nucleus scattering*, *Phys. Rev.* **D 96** (2017) 095007 [arXiv:1612.06350] [INSPIRE].

[27] Y. Cui, M. Pospelov and J. Pradler, *Signatures of dark radiation in neutrino and dark matter detectors*, *Phys. Rev.* **D 97** (2018) 103004 [arXiv:1711.04531] [INSPIRE].

[28] D. Aristizabal Sierra, N. Rojas and M.H.G. Tytgat, *Neutrino non-standard interactions and dark matter searches with multi-ton scale detectors*, *JHEP* **03** (2018) 197 [arXiv:1712.09667] [INSPIRE].

[29] S.-F. Ge and I.M. Shoemaker, *Constraining photon portal dark matter with Texono and coherent data*, arXiv:1710.10889 [INSPIRE].

[30] Y. Farzan, *A model for large non-standard interactions of neutrinos leading to the LMA-Dark solution*, *Phys. Lett.* **B 748** (2015) 311 [arXiv:1505.06906] [INSPIRE].

[31] Y. Farzan and J. Heeck, *Neutrinophilic nonstandard interactions*, *Phys. Rev.* **D 94** (2016) 053010 [arXiv:1607.07616] [INSPIRE].

[32] W. Rodejohann, X.-J. Xu and C.E. Yaguna, *Distinguishing between Dirac and Majorana neutrinos in the presence of general interactions*, *JHEP* **05** (2017) 024 [arXiv:1702.05721] [INSPIRE].

[33] D.Z. Freedman, *Coherent neutrino nucleus scattering as a probe of the weak neutral current*, *Phys. Rev.* **D 9** (1974) 1389 [INSPIRE].

[34] G. Bélanger, F. Boudjema, A. Pukhov and A. Semenov, *Dark matter direct detection rate in a generic model with MicrOMEGAs* 2.2, *Comput. Phys. Commun.* **180** (2009) 747 [arXiv:0803.2360] [INSPIRE].

[35] A. Crivellin, M. Hoferichter and M. Procura, *Accurate evaluation of hadronic uncertainties in spin-independent WIMP-nucleon scattering: disentangling two- and three-flavor effects*, *Phys. Rev.* **D 89** (2014) 054021 [arXiv:1312.4951] [INSPIRE].

[36] M. Hoferichter, J. Ruiz de Elvira, B. Kubis and U.-G. Meißner, *High-precision determination of the pion-nucleon σ term from Roy-Steiner equations*, *Phys. Rev. Lett.* **115** (2015) 092301 [arXiv:1506.04142] [INSPIRE].

JHEP05(2018)066

[37] P. Junnarkar and A. Walker-Loud, *Scalar strange content of the nucleon from lattice QCD*, *Phys. Rev.* **D 87** (2013) 114510 [arXiv:1301.1114] [INSPIRE].

[38] M.A. Shifman, A.I. Vainshtein and V.I. Zakharov, *Remarks on Higgs boson interactions with nucleons*, *Phys. Lett.* **B 78** (1978) 443 [INSPIRE].

[39] J.M. Alarcon, L.S. Geng, J. Martin Camalich and J.A. Oller, *The strangeness content of the nucleon from effective field theory and phenomenology*, *Phys. Lett.* **B 730** (2014) 342 [arXiv:1209.2870] [INSPIRE].

[40] J.M. Alarcon, J. Martin Camalich and J.A. Oller, *The chiral representation of the πN scattering amplitude and the pion-nucleon sigma term*, *Phys. Rev.* **D 85** (2012) 051503 [arXiv:1110.3797] [INSPIRE].

[41] Particle Data Group collaboration, C. Patrignani et al., *Review of particle physics*, *Chin. Phys.* **C 40** (2016) 100001 [INSPIRE].

[42] Y. Kamiya, K. Itagami, M. Tani, G.N. Kim and S. Komamiya, *Constraints on new gravitylike forces in the nanometer range*, *Phys. Rev. Lett.* **114** (2015) 161101 [arXiv:1504.02181] [INSPIRE].

[43] Yu. N. Pokotilovski, *Constraints on new interactions from neutron scattering experiments*, *Phys. Atom. Nucl.* **69** (2006) 924 [hep-ph/0601157] [INSPIRE].

[44] H. Leeb and J. Schmiedmayer, *Constraint on hypothetical light interacting bosons from low-energy neutron experiments*, *Phys. Rev. Lett.* **68** (1992) 1472 [INSPIRE].

[45] P.S. Pasquini and O.L.G. Peres, *Bounds on neutrino-scalar Yukawa coupling*, *Phys. Rev.* **D 93** (2016) 053007 [*Erratum ibid.* **D 93** (2016) 079902] [arXiv:1511.01811] [INSPIRE].

[46] W. Rodejohann, *Neutrino-less double beta decay and particle physics*, *Int. J. Mod. Phys.* **E 20** (2011) 1833 [arXiv:1106.1334] [INSPIRE].

[47] KamLAND-Zen collaboration, A. Gando et al., *Limits on Majoron-emitting double-β decays of ^{136}Xe in the KamLAND-Zen experiment*, *Phys. Rev.* **C 86** (2012) 021601 [arXiv:1205.6372] [INSPIRE].

[48] M. Agostini et al., *Results on $\beta\beta$ decay with emission of two neutrinos or Majorons in ^{76}Ge from GERDA phase I*, *Eur. Phys. J.* **C 75** (2015) 416 [arXiv:1501.02345] [INSPIRE].

[49] G.G. Raffelt, *Stars as laboratories for fundamental physics*, http://wwwth.mpp.mpg.de/members/raffelt/mypapers/199613.pdf, (1996).

[50] G.-Y. Huang, T. Ohlsson and S. Zhou, *Observational constraints on secret neutrino interactions from big bang nucleosynthesis*, *Phys. Rev.* **D 97** (2018) 075009 [arXiv:1712.04792] [INSPIRE].

[51] Planck collaboration, P.A.R. Ade et al., *Planck* 2015 *results. XIII. Cosmological parameters*, *Astron. Astrophys.* **594** (2016) A13 [arXiv:1502.01589] [INSPIRE].

[52] M.E. Peskin and D.V. Schroeder, *An introduction to quantum field theory*, Addison-Wesley, Reading U.S.A., (1995) [INSPIRE].

[53] S. Bergmann, Y. Grossman and E. Nardi, *Neutrino propagation in matter with general interactions*, *Phys. Rev.* **D 60** (1999) 093008 [hep-ph/9903517] [INSPIRE].

[54] V.I. Kopeikin, *Flux and spectrum of reactor antineutrinos*, *Phys. Atom. Nucl.* **75** (2012) 143 [*Yad. Fiz.* **75** (2012) 165] [INSPIRE].

JHEP05(2018)066

[55] P. Coloma, P.B. Denton, M.C. Gonzalez-Garcia, M. Maltoni and T. Schwetz, *Curtailing the dark side in non-standard neutrino interactions*, *JHEP* **04** (2017) 116 [arXiv:1701.04828] [INSPIRE].

[56] P. Bakhti and Y. Farzan, *Constraining secret gauge interactions of neutrinos by meson decays*, *Phys. Rev.* **D 95** (2017) 095008 [arXiv:1702.04187] [INSPIRE].

[57] S.-F. Ge, M. Lindner and W. Rodejohann, *Atmospheric trident production for probing new physics*, *Phys. Lett.* **B 772** (2017) 164 [arXiv:1702.02617] [INSPIRE].

[58] K. Blum, A. Hook and K. Murase, *High energy neutrino telescopes as a probe of the neutrino mass mechanism*, arXiv:1408.3799 [INSPIRE].

JHEP05(2018)066